Table IV. Dihedral Angles and Least-Squares Planes for
$[VO(O_2C_6H_2(t\text{-Bu})_2)_2]_2$

Dihedral Angles

plane 1	plane 2	angle, deg
O(1)–V–O(2)	bridging ligand	24.0
O(3)–V–O(4)	chelating ligand	7.6

Least-Squares Planes

atom	deviation, Å	atom	deviation, Å
Bridging Ligand, $4.52x + 3.90y - 11.02z = +0.48$			
V	−0.646	C(3)	0.005 (7)
O(1)	−0.013 (5)	C(4)	0.018 (8)
O(2)	0.000 (5)	C(5)	−0.007 (8)
C(1)	0.024 (7)	C(6)	0.015 (8)
C(2)	0.004 (7)		
Chelating Ligand, $5.89x - 9.18y + 8.08z = -1.67$			
V	−0.196	C(17)	0.010 (8)
O(3)	−0.002 (5)	C(18)	0.023 (9)
O(4)	0.016 (5)	C(19)	0.011 (8)
C(15)	−0.017 (7)	C(20)	−0.028 (8)
C(16)	−0.021 (7)		

graphite crystal monochromator. The centered settings of 15 reflections were used to calculate the cell constants given in Table I. Data were collected at ambient room temperature out to a 2θ value of 45° by using Mo Kα radiation. Standards monitored during data collection showed no significant variation in intensity.

The structure was solved by using standard heavy-atom procedures. Both the complex molecule and the anisole solvate molecule are located about centers of inversion. This results in disorder of the methoxy group of the solvent. Additionally, one *t*-Bu group of the complex was found to have twofold disorder resulting in six half-atom positions for the methyl carbon atoms. These were treated accordingly. The structure was refined by using programs and procedures described previously.[29] Fixed corrections were applied for the hydrogen atoms of the molecules. The final cycle of refinement converged with $R_F = 0.064$ and $R_{wF} = 0.068$. The standard deviation of an observation of unit weight was 1.84. Final positional and thermal parameters and their estimated standard deviations are listed in Table II. Values of F_o and F_c (×10) are available as supplementary material.

Registry No. V(3,5-DBSQ)$_3$, 64020-88-8; [VO(3,5-DBSQ)(3,5-DBCat)]$_2$, 84850-87-3; [VO(O$_2$C$_6$H$_2$(*t*-Bu)$_2$)$_2$]$_2$;C$_6$H$_5$OCH$_3$, 84894-07-5; V(CO)$_6$, 14024-00-1; VO(acac)$_2$, 3153-26-2.

Supplementary Material Available: Tables of observed and calculated structure factors (7 pages). Ordering information is given on any current masthead page.

(29) Pierpont, C. G. *Inorg. Chem.* **1977**, *16*, 636–639.

Metal–Metal Multiple Bonds. 10. Electrophilic Additions of Halogens and Hydrogen Halides to the Mo–Mo Triple Bond in Cp2Mo2(CO)4[1]

M. David Curtis,* Nicephoros A. Fotinos, Kyoung R. Han, and William M. Butler

Contribution from the Department of Chemistry, The University of Michigan, Ann Arbor, Michigan 48109. Received August 12, 1982

Abstract: The synthesis of Cp$_2$Mo$_2$(CO)$_4$(μ-Cl)(Cl) (**6**), Cp$_2$Mo$_2$(CO)$_4$(μ-H)(μ-I) (**8**), and Cp$_2$Mo$_2$(CO)$_4$(μ-I)$_2$ (**2**) is described. Complex **6** is best prepared from Cp$_2$Mo$_2$(CO)$_4$ (**1**) and PhICl$_2$ or HCl in toluene. Complex **8** is formed from **1** and HI. Excess HI converts **8** to the diiodide **2**. Reaction of **2** with aluminum hydrides gives **8**, which in turn reacts to give H$_2$ and **1**. The XPS of **6** shows two types of chlorine in a 1:1 ratio with 2P$_{3/2}$ ionization energies of 198.8 and 197.6 eV consistent with bridging and terminal positions, respectively. The different geometrical isomers that are exhibited by the dihalides are discussed. The structures of **2** and **8** were determined by X-ray crystallography. For **2**, the violet isomer forms crystals in the triclinic system, $a, b, c = 6.882$ (1), 10.196 (2), 6.856 (1) Å; $\alpha, \beta, \gamma = 86.08$ (1), 113.83 (1), 102.52 (1)°, $V = 429.5$ (1) Å^3, $Z = 1$, space group $P\bar{1}$, ρ(calcd) = 2.62 g/cm^3. The structure was refined with 1702 reflections with $I > 3\sigma(I)$. The final R values are $R_1 = 0.027$, $R_2 = 0.039$. Some selected interatomic distances are Mo–I = 2.853 (1) Å, Mo···Mo = 4.441 Å, and I···I = 3.581 (1) Å. Selected bond angles are IMoI = 77.76 (2)° and MoIMo = 102.24 (2)°. The HI adduct, **8**, crystallizes in the monoclinic system: $a, b, c = 9.321$ (3), 15.131 (6), 11.394 (4) Å; $\beta = 97.94$ (3)°; $V = 1592$ (1) Å^3, $Z = 4$, space group $P2_1/n$, ρ(calcd) = 2.25; ρ(obsd) = 2.34 g/cm^3. The structure was refined with 2647 reflections with $I > 3\sigma(I)$ to final R values of $R_1 = 0.063$ and $R_2 = 0.073$. The bridging hydrogen was not located. Selected interatomic distances (Å) and bond angles follow: Mo–Mo = 3.310 (2), Mo–I = 2.760 (1); MoIMo = 73.70 (4), IMoMo = 53.15 (av). The nature of the bridging Mo(μ-H)(μ-X)Mo system is discussed in an EHMO framework, and the significant tilt of the Cp groups is ascribed to a trans influence propagated in the σ(Mo–CO) and π(Mo–Cp) bonding orbitals.

The discovery of the reactivity patterns of metal–metal multiple bonds is an area of considerable current interest.[2,3] The two compounds that have received the most attention in this regard are Cp$_2$Mo$_2$(CO)$_4$[2a] and Mo$_2$X$_6$ (X = OR, NR$_2$).[2b] Both of these complexes add nucleophiles and both undergo two-center oxidative addition reactions. The reaction of M≡M triple bonds with halogens and hydrogen halides is of special interest. This interest derives from two sources. First, halogenations and hydrohalogenations of carbon–carbon multiple bonds are important reactions since new functional groups are introduced while the carbon–carbon skeleton is maintained. The resulting halides are in turn useful precursors to a variety of compounds. Can metal–metal multiple bonds serve as inorganic functional groups in the same fashion? Second, the reactivity of dimetal centers, especially multiply bonded centers, has not been systematized,
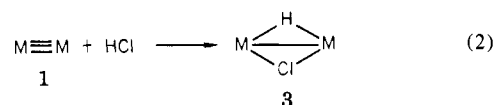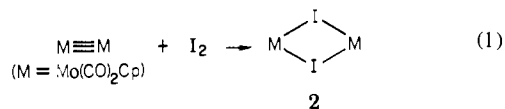
(1) Part 9: Messerle, L.; Curtis, M. D. *J. Am. Chem. Soc.* **1980**, *104*, 889.

(2) For leading reviews, see: (a) Curtis, M. D.; Messerle, L.; Fotinos, N. A.; Gerlach, R. F. *ACS Symp. Ser.* **1981**, *No. 155*, 221–257. (b) Chisholm, M. H. *Ibid.* **1981**, *No. 155*, 17–39. (c) Walton, R. A. *Ibid.* **1981**, *No. 155*, 207–220.

(3) Cotton, F. A.; Walton, R. A. "Multiple Bonds Between Metal Atoms"; Wiley: New York, 1982.

and therefore even theoretical treatments must approach the problem piecemeal. Halogenation and hydrohalogenation provide handy comparisons to their well-developed organic analogues.

The availability of variable coordination modes, bridged vs. unbridged forms,[4-6] and multicenter bonding renders the chemistry of multiply bonded dimetal centers more complex than the corresponding carbon chemistry. Curtis and Klingier first reported on the halogenation and hydrohalogenation of the Mo≡Mo triple bond in $Cp_2Mo_2(CO)_4$ (**1**) (eq 1 and 2).[7] The diiodide was

$$M\equiv M + I_2 \longrightarrow M\overset{I}{\underset{I}{\diamond}}M \quad (1)$$
$$(M = Mo(CO)_2Cp)$$
$$\mathbf{2}$$

$$M\equiv M + HCl \longrightarrow M\overset{H}{\underset{Cl}{\diamond}}M \quad (2)$$
$$\mathbf{1} \qquad\qquad\qquad \mathbf{3}$$

reported to form two isomers, a red-brown form isolated from the low-temperature reaction of I_2 with **1** and a violet isomer, which is formed when solutions of the red-brown form are warmed to room temperature. Chisholm et al.[8] have demonstrated that both halogens and organic peroxides oxidatively add to the Mo≡Mo triple bond of $Mo_2(OR)_6$ complexes. During these reactions, the metal–metal bond order is reduced from 3 to 1 and two of the initially terminal alkoxides assume bridge positions.

Glicksman and Walton found that the addition of HI and I⁻ to $Mo_2(OAc)_4$ (Mo⁴Mo) gave the cluster anion $Mo_4I_{11}{}^{2-}$.[9] Recently, Sattelberger et al. have shown that H_2, HCl, and Cl_2 add to the dinuclear tantalum complex $Ta_2(PMe_3)_4Cl_6$ (Ta=Ta) to give the corresponding adducts in which the two added atoms assume bridging positions and the Ta–Ta bond order is reduced from 2 to 1.[10] Oxidative addition to d^8 dimers can also be used to *increase* the formal bond order from 0 to 1.[11]

The above examples suffice to indicate the complexity of oxidative additions to dinuclear centers. The present work was undertaken to gain a better understanding of the factors that influence bridge–terminal interchanges of ligands in dinuclear centers and to gain further knowledge of structure–reactivity relationships in multiply bonded metal–metal dimers.

Results and Discussion

Synthesis and Characterization. One of the interesting properties of the diiodide $Cp_2Mo_2(CO)_4I_2$ (**2**) is its isomerization in solution. This isomerization may be followed by NMR. At −65 °C in C_7D_8, the low-temperature form exhibits a single Cp resonance at δ 5.57. Warming the solution briefly to 0 °C causes a diminution of the original signal intensity and the appearance of a new signal at δ 5.51. Repeating the warm–cool cycle causes the δ 5.57 signal to gradually be replaced by the δ 5.51 signal and the color of the solution changes from red brown to violet. An isomerization of the type shown in eq 3 was suggested to explain these results.[7]

$$\overset{I}{\underset{I}{M=M}} \rightleftarrows M\overset{I}{\underset{I}{\diamond}}M \quad (3)$$
$$\mathbf{2a} \qquad\qquad \mathbf{2}$$
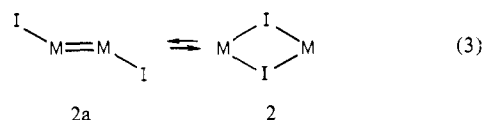
(4) Shaik, S.; Hoffmann, R. *J. Am. Chem. Soc.* **1980**, *102*, 1194.
(5) Jemmis, E. D.; Pinhas, A. R.; Hoffmann, R. *J. Am. Chem. Soc.* **1980**, *102*, 2576.
(6) Shaik, S.; Hoffmann, R.; Fisel, C. R.; Summerville, R. H. *J. Am. Chem. Soc.* **1980**, *102*, 4555.
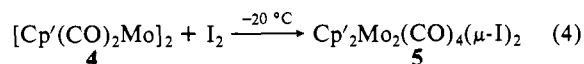(7) Curtis, M. D.; Klingler, R. J. *J. Organomet. Chem.* **1978**, *161*, 23.
(8) Chisholm, M. H.; Kirkpatrick, C. C.; Huffman, J. C. *Inorg. Chem.* **1981**, *20*, 871.
(9) Glicksman, H. D.; Walton, R. A. *Inorg. Chem.* **1978**, *17*, 3197.
(10) Wilson, R. B., Jr.; Sattelberger, A. P.; Huffman, J. C. *J. Am. Chem. Soc.* **1982**, *104*, 858.
(11) For a list of leading references, see: Coleman, A. W.; Eadie, D. T.; Stobart, S. R.; Zaworotke, M. J.; Atwood, J. L. *J. Am. Chem. Soc.* **1982**, *104*, 922.

A note in ref 7 states that the low-temperature isomer has structure **2**. The crystals used for the structure determination were grown by allowing a saturated solution of the low-temperature, red-brown isomer to stand in contact with the red-brown solid at −10 °C for 10 days, and it was assumed that the crystals so obtained were those of the low-temperature form (the larger crystals are so dark that it is difficult to discern their color). Since then we have obtained identical crystals from violet solutions of the high temperature form. Apparently, on standing for 10 days, enough isomerization had occurred to give the violet isomer, which formed the crystals used in the structure determination. Therefore, the initial assertion is in error and the violet isomer has the $(\mu\text{-}I)_2$ structure represented by **2**. The methyl-substituted diiodide was prepared as shown in eq 4 ($Cp' = C_5H_4Me$) with the hope that

$$[Cp'(CO)_2Mo]_2 + I_2 \xrightarrow{-20\ °C} Cp'_2Mo_2(CO)_4(\mu\text{-}I)_2 \quad (4)$$
$$\mathbf{4} \qquad\qquad\qquad\qquad \mathbf{5}$$

the increased solubility would allow us to grow larger crystals of the low-temperature, red-brown isomer. When the reaction shown in (4) was conducted in an NMR tube at −30 °C (C_7D_8 solvent), the resonances due to **4** (Cp δ 4.74, A_2B_2 pattern with $\Delta\delta$ = 7.8 Hz, J_{AB} = 2.2 Hz; and Me δ 1.92) were gradually replaced with new resonances at δ 4.61 (Cp, A_2B_2 with $\Delta\delta$ = 30.5 Hz, J_{AB} = 2.1 Hz) and δ 2.03 (Me). These new signals are identical with those observed for authentic $Cp'_2Mo_2(CO)_4(\mu\text{-}I)_2$ (see Experimental Section) at −30 °C. It is concluded that the methylcyclopentadienyl complex does not exhibit a low-temperature isomer as observed for **2**. Therefore, it is likely that the less soluble, red-brown isomer of **2** is a kinetically controlled product that is "trapped" by precipitation at −30 °C.

In light of the odd behavior exhibited by the diiodide adducts, it was of considerable interest to probe the behavior of another member of this class of compounds. Accordingly, we set out to synthesize the dichloride **6**. Chlorine gas reacts rapidly with **1** at −78 °C to give a complex reaction mixture that contains $CpMo(CO)_3Cl$, $CpMo(CO)_2Cl_3$, and approximately 10% of the desired dichloride dimer, **6** (eq 5).

$$M\equiv M + Cl_2 \xrightarrow{-78\ °C} CpMo(CO)_3Cl + CpMo(CO)_2Cl_3 +$$
$$Cp_2Mo_2(CO)_4(\mu\text{-}Cl)Cl + ... \quad (5)$$
$$\mathbf{6}$$
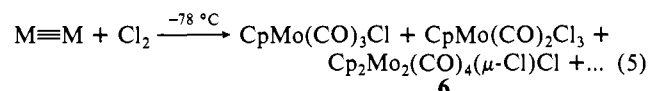
A much better route to complex **6** utilizes the mild Cl_2-transfer agent phenyliodonium dichloride, $PhICl_2$. This reagent reacts with **1** in toluene at −50 °C to give an insoluble brown solid and a dark solution from which complex **6** is isolated in ca. 40% yield.

Unlike the diiodide **2**, complex **6** exhibits two Cp singlets in the ¹H NMR spectrum at δ 4.95 and 4.92. The IR spectrum of **6** in the ν_{CO} region (KBr) (1995, 1940, 1900, and 1855 (sh) cm⁻¹) is also more complex than that of **2** (1960, 1945, 1870 (sh) cm⁻¹), consistent with a lower symmetry for **6** vis-à-vis **2**.

The XPS spectrum of solid **6** was kindly recorded by Prof. R. E. McCarley and M. Luly of the Department of Chemistry, Iowa State University. The chlorine $2p_{3/2,1/2}$ spectrum is shown in Figure 1. The observed spectrum (crosses in Figure 1) is nicely fitted by two types of Cl at 198.83 and 197.56 eV (vs. C (1s) at 285.0 eV). Each Cl peak is a $2p_{3/2,1/2}$ doublet with a $^3/_2 - ^1/_2$ separation of 1.55 eV. The 1.27-eV difference in the 2p ioniztion energies is consistent with the presence of bridging and terminal chloride ligands in the complex.[12,13] The fitted area ratios of the two components are 1.00:1.01. The reaction of **1** with $PhICl_2$ is therefore described by eq 6 and the structure of **6** is proposed as shown.

$$M\equiv M + PhICl_2 \longrightarrow PhI + Cp(CO)_2Mo\overset{Cl}{\underset{Cl}{\diamond}}Mo(CO)_2Cp \quad (6)$$
$$\mathbf{6}$$
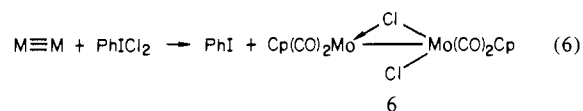
(12) Best, S. A.; Walton, R. A. *Inorg. Chem.* **1979**, *18*, 484.
(13) Ebner, J. R.; McFadden, D. L.; Tyler, D. R.; Walton, R. A. *Inorg. Chem.* **1976**, *15*, 3014.
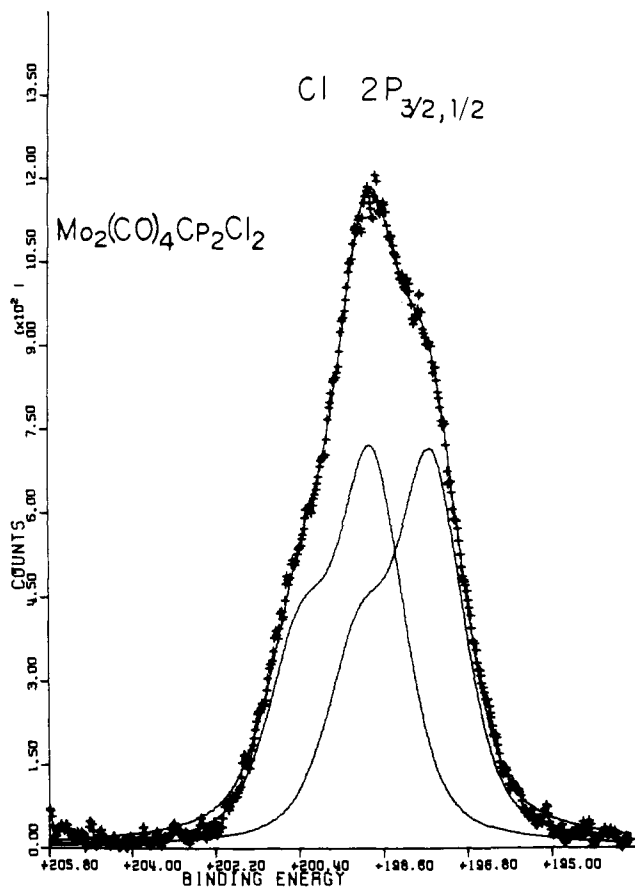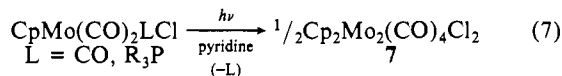
2688 *J. Am. Chem. Soc., Vol. 105, No. 9, 1983*

Curtis et al.

Figure 1. X-ray photoelectron spectrum of the Cl $2p_{3/2,1/2}$ binding energies. Crosses are experimental points: the two inner curves are the least-squares fitted curves for the two types of chlorine, whose sum gives the line through the experimental points.

In the proposed structure of **6**, one molybdenum is formally Mo(I) and the other is formally Mo(III). Both achieve the 18-electron count via the bridging chloride and metal–metal bond. In spite of the different formal oxidation states, only one set of Mo $3d_{5/2,3/2}$ peaks were observed in the Mo XPS spectrum of **6** at 228.75 and 231.92 eV, respectively. The lack of splitting of the Mo 3d spectrum into the expected two components is also consistent with previous experience.[12-14]

Another complex with the formula, $Cp_2Mo_2(CO)_4Cl_2$, has been synthesized by Ali et al.[15,16] by the route shown in eq 7. Complex

$$CpMo(CO)_2LCl \xrightarrow[\substack{pyridine \\ (-L)}]{h\nu} {}^1/_2Cp_2Mo_2(CO)_4Cl_2 \qquad (7)$$
$$L = CO, R_3P$$
$$\phantom{CpMo(CO)_2LCl \xrightarrow[\substack{pyridine}]{h\nu} {}^1/_2Cp_2Mo_2(CO)_4Cl_2}\mathbf{7}$$

7 is described as being dark red, as having ν_{CO} bands at 1955 and 1858 cm^{-1}, and as exhibiting one resonance for the Cp group at δ 5.8. The structure of **7** is probably analogous to that of the bridging diiodide, **2**.[17] It is significant that we have been unable to observe any **7** in our reactions of M$\equiv$M (**1**) with chlorinating agents, nor have we observed the rearrangement of **6** into **7** under any conditions.

(14) A referee suggested an alternate formalism for **6**

$$M \xleftarrow{} M\!\!-\!\!Cl$$
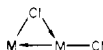
which involves a Mo$\rightarrow$Mo dative bond between two Mo(II) centers, and claimed this formalism is more easily reconciled with the lack of resolution of the Mo(3d) peaks in the XPS. However, a dative Mo$\rightarrow$Mo bond would put *formal* charges of ±1 on the two molybdenums. Hence both formalisms predict a higher charge on the molybdenum bonded to two chlorines.

(15) Ali, L. H.; Cox, A.; Kemp, T. J. *J. Chem. Soc., Dalton Trans.* **1973**, 1475.

(16) Allen, D. M.; Cox, A.; Kemp, T. J.; Ali, L. H. *J. Chem. Soc., Dalton Trans.* **1973**, 1899.

(17) We are continuing our efforts to grow crystallography grade crystals of the red-brown isomers of **2** and both forms of the dichlorides **6** and **7**.

Hydrogen iodide reacts with the Mo$\equiv$Mo triple bond in **1** to form an HI adduct (**8**), which is much more stable than the previously reported HCl adduct. A crystal structure (see below) has established the (μ-H)(μ-I) formulation shown in eq 8 (M = Cp(CO)$_2$Mo). Complex **8** shows one Cp resonance in the proton
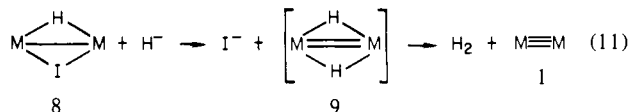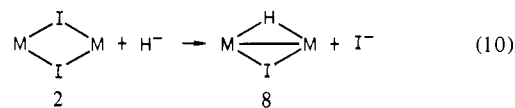
$$M\equiv M + HI \longrightarrow M\diagdown\!\!\!\!\diagup M \qquad (8)$$
$$\mathbf{8}$$
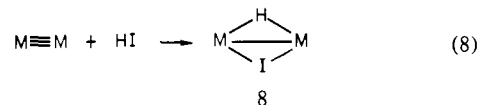
NMR spectrum at δ 4.72 and the bridging hydride appears at δ -11.45. The carbonyl stretches occur at 1940 and 1855 cm^{-1}.

Complex **8** reacts with excess HI to give the bridging diiodide, **2** (eq 9). The sequence may be reversed by adding a hydride

$$M\diagup\!\!\!\!\diagdown M + HI \longrightarrow H_2 + M\diagup\!\!\!\!\diagdown M \qquad (9)$$
$$\mathbf{8} \qquad\qquad\qquad \mathbf{2}$$
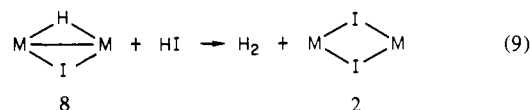
source, e.g., LiAl(H)(O-*t*-Bu)$_3$, to the diiodide **2**. One equivalent of hydride gives **8**, while 2 equiv (or 1 equiv of H$^-$ + **8**) regenerates the M$\equiv$M triple bond (eq 10 and 11). The decomposition of

$$M\diagup\!\!\!\!\diagdown M + H^- \longrightarrow M\diagup\!\!\!\!\diagdown M + I^- \qquad (10)$$
$$\mathbf{2} \qquad\qquad\qquad \mathbf{8}$$

$$M\diagup\!\!\!\!\diagdown M + H^- \longrightarrow I^- + \left[M\diagup\!\!\!\!\diagdown M\right] \longrightarrow H_2 + M\equiv M \qquad (11)$$
$$\mathbf{8} \qquad\qquad\qquad\quad \mathbf{9} \qquad\qquad\qquad \mathbf{1}$$

the presumed dihydride, **9**, into H$_2$ and **1** is consistent with the observation that **1** does not react with H$_2$ under normal conditions; i.e., the equilibrium, **9** $\rightleftarrows$ H$_2$ + **1**, lies far to the right.

The amphoteric nature of the bridging hydride in **8** is demonstrated by the set of reactions 8–11. In eq 8, the bridging hydrogen is introduced as a proton, but it reacts as a hydride ion in eq 9. In eq 10, the bridging hydrogen is introduced as a hydride ion, but it reacts as a proton in eq 11.

Armed with the knowledge that **8** reacts further with HI to give the diiodide, we reinvestigated the reaction of **1** with HCl. The conditions under which the complex Cp$_2$Mo$_2$(CO)$_4$(μ-H)(μ-Cl) (**3**) can be isolated even in moderate yields are quite specific.[7] It turns out that one reason for the low to moderate yields of **3** is that this complex also reacts rapidly with excess HCl to form the dichloride, **6**, identical in all respects with that made from Cl$_2$ or PhICl$_2$ and **1** (cf. eq 5, 6, and 12, M = Mo(CO)$_2$Cp). In

$$M\diagup\!\!\!\!\diagdown M + HCl \longrightarrow H_2 + M\diagup\!\!\!\!\diagdown M \qquad (12)$$
$$\mathbf{3} \qquad\qquad\qquad\qquad \mathbf{6}$$
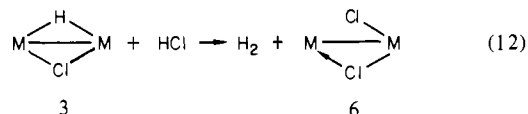
addition, brown, insoluble, non-carbonyl-containing substances are also produced.

Reactions. The violet form of the diiodide **2** has been shown to react with triphenylphosphine or carbon monoxide according to eq 13 (L = Ph$_3$P or CO).[18] For L = Ph$_3$P, refluxing the

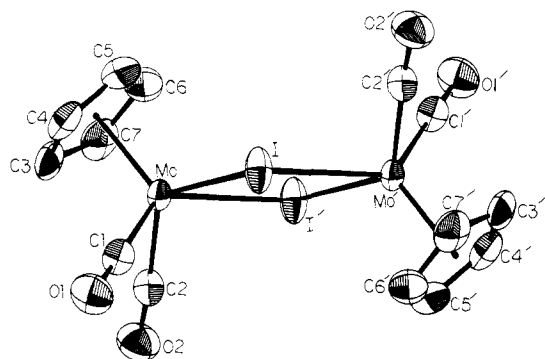$$Cp_2Mo_2(CO)_4I_2 + 2L \longrightarrow 2 CpMo(CO)_2IL \qquad (13)$$
$$\mathbf{2}$$
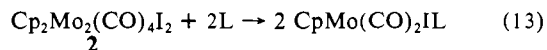
reactants in toluene for 1 h gave complete conversion, whereas 1 h at room temperature ($P = 1$ atm) sufficed for complete conversion with L = CO. The resulting CpMo(CO)$_2$(PPh$_3$)I is approximately a 50:50 mixture of cis and trans isomers as determined from both IR and NMR.[19] Thus, the iodide-bridged complex **2** should be a useful precursor to a variety of CpMo-

(18) Klingler, R. J. Ph.D. Thesis, The University of Michigan, Ann Arbor, MI, 1977.

(19) Spectral properties of both *cis*- and *trans*-CpMo(CO)$_2$(PPh$_3$)I have been reported: Manning, A. R. *J. Chem. Soc. A* **1967**, 1984.

Table I. Crystal and Data Collection Summary for $Cp_2Mo_2(CO)_4I_2$

a, b, c, Å	6.882 (1), 10.196 (2), 6.856 (1)
α, β, γ, deg	86.08 (1), 113.83 (1), 102.52 (1)
V, Å^3; Z	429.5 (1); 1
ρ(calcd), g/cm^3	2.62
crystal dimensions, mm	0.12 × 0.03 × 0.22
radiation	Mo Kα, monochromatized from a graphite crystal
take-off angle, deg	4
μ, cm^{-1}	50.05
transmission factors, max/min	0.91/0.56
scan speed, deg/min	2–15
std reflections	01$\bar{3}$, 21$\bar{1}$, 1$\bar{1}$1
2θ limit, deg	55
total reflections	2113
reflections with $I > 3\sigma$	1702
std deviation of an observation of unit weight	1.41
R_1, R_2	0.027, 0.039

Figure 3. Perspective view of one end of the $Cp_2Mo_2(CO)_4(\mu$-I$)_2$ molecule up the Mo–Cp (centroid) axis.

Figure 2. ORTEP II plot of $Cp_2Mo_2(CO)_4(\mu$-I$)_2$ (**2**) showing the atomic numbering scheme.

Figure 4. ORTEP II plot of the structure of $Cp_2Mo_2(CO)_4(\mu$-H$)(\mu$-I$)$ (**8**) showing the atomic numbering scheme. The hydrogen, believed to lie on a pseudo-C_2 axis passing through the iodine and the Mo–Mo midpoint, was not located.

$(CO)_2XI$ complexes in the same manner as the halide-bridged dimers of Rh(I), Ir(I), and Pt(II) serve as useful precursors for substitution reactions on these group 8 metals.

In contrast, the $(\mu$-H$)(\mu$-I$)$ derivative, **8**, does not react with CO under 4 atm pressure at 70 °C. Complex **8** was likewise inert to mixtures of H_2 and CO or H_2 alone under similar conditions.

The possible reactions of **8** with terminal olefins is of special interest since one can draw a reasonable scheme for binuclear catalysis of anti-Markovnikov addition of HX to terminal olefins.[20,21] At room temperature, there was no reaction between **8** and 1-hexene after 20 h. Heating the mixture to 70 °C for 5 h resulted in the complete conversion of the 1-hexene to a mixture of 2- and 3-hexenes, but the NMR signal due to **8** had retained >95% of its original intensity.

The reaction of **8** with ethylene follows a different course. The only organic product formed is 3-pentanone (38% based on **8**). Bergman and Jones[22] have noted that $CpMo(CO)_3H$ reacts with ethylene to form 3-pentanone, **1**, and $Cp_2Mo_2(CO)_6$. However, the extent of decomposition of **8** to $CpMo(CO)_3H$ is insufficient to account for the amount of 3-pentanone observed.
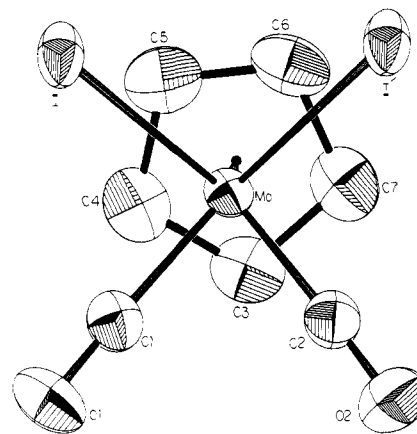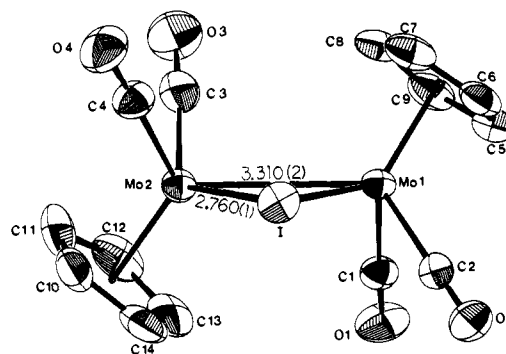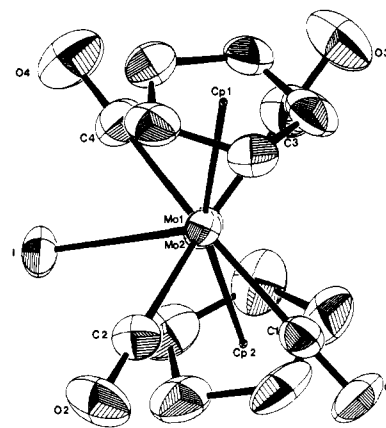
Structures. Crystals of the diiodide **2** were grown by allowing a saturated solution to stand in contact with excess red-brown solid at −10 °C for 10 days. We have since obtained identical crystals from solutions of the violet isomer at room temperature. Therefore, the structure reported here is of the violet, high-temperature form.

Table I lists the crystal and data collection statistics. In Table II are the fractional atomic coordinates and temperature factors.

Figure 5. Perspective view of the structure of **8** was viewed down the Mo1–Mo2 axis.

The derived bond distances and angles are given in Tables III and IV. Figure 2 is an ORTEP II plot of the molecule showing the numbering scheme, and Figure 3 is a perspective view of the "four-legged piano stool" arrangement of the ligands, looking up the Mo–Cp axis.

The crystal and data collection summary for the structure determination of the HI adduct **8** is given in Table V, the atomic coordinates in Table VI, and the temperature factors in Table VII. Tables VIII and IX display selected bond distances and angles. The atomic numbering scheme is shown in Figure 4, and the molecular structure of **8** as viewed down the Mo–Mo axis is shown in Figure 5.

The diiodide has crystallographically imposed C_i symmetry, but the actual symmetry closely approximates C_{2h}. The hydriodide **8** has no imposed symmetry, but there is an approximate C_2 axis

(20) Curtis, M. D.; Han, K. R.; Klingler, R. J. "Proceedings of the 3rd International Conference of Chemistry and Uses of Molybdenum"; Barry, H. F., Mitchell, P. C. F., Eds.; Climax Molybdenum Co.: Ann Arbor, MI, 1979; pp 39–44.

(21) It was reported (ref 18, 20) that HCl(g) reacted with 1-hexene in the presence of **1** to give an amount of 1-chlorohexane approximately equivalent to the quantity of **1** present in the mixture. We have been unable to repeat this observation under a variety of conditions.

(22) Jones, W. D.; Bergman, R. G. *J. Am. Chem. Soc.* **1979**, *101*, 5447.

Table II. Fractional Cell Coordinates and Anisotropic Temperature Factors for $Cp_2Mo_2(CO)_4I_2$ (Violet Isomer)[a]

atom	x	y	z	atom	x	y	z
Mo	0.01581 (6)	0.21199 (4)	-0.10275 (6)	C3	0.0137 (10)	0.3847 (6)	-0.3256 (9)
I	0.28930 (5)	0.03387 (3)	0.13935 (6)	C4	0.2110 (10)	0.3420 (6)	-0.2762 (9)
C1	0.2103 (8)	0.3264 (5)	0.1463 (8)	C5	0.1602 (11)	0.2140 (7)	-0.3697 (10)
O1	0.3227 (8)	0.3985 (5)	0.2888 (7)	C6	-0.0671 (11)	0.1727 (6)	-0.4710 (9)
C2	-0.1788 (8)	0.2756 (5)	-0.0073 (9)	C7	-0.1613 (10)	0.2779 (7)	-0.4431 (9)
O2	-0.2907 (7)	0.3208 (5)	0.0454 (8)				

atom	B_{11}	B_{22}	B_{33}	B_{12}	B_{13}	B_{23}	B[b]
Mo	2.50 (2)	1.85 (2)	2.31 (2)	0.38 (1)	0.82 (1)	0.43 (1)	2.23 (1)
I	2.16 (1)	2.46 (2)	5.26 (2)	0.34 (1)	0.74 (1)	1.04 (1)	3.12 (1)
C1	3.2 (2)	3.2 (2)	3.2 (2)	0.4 (2)	1.2 (2)	0.4 (2)	3.3 (1)
O1	5.3 (2)	4.7 (2)	3.7 (2)	-0.1 (2)	0.9 (2)	-1.4 (2)	4.6 (1)
C2	3.1 (2)	2.7 (2)	3.7 (2)	0.5 (2)	1.2 (2)	0.3 (2)	3.2 (1)
O2	4.7 (2)	5.0 (2)	6.0 (2)	1.7 (2)	2.6 (2)	-0.2 (2)	4.8 (1)
C3	5.7 (3)	3.1 (2)	3.1 (2)	0.9 (2)	1.9 (2)	1.4 (2)	3.5 (1)
C4	4.5 (3)	4.3 (3)	3.7 (2)	-0.0 (2)	2.3 (2)	1.1 (2)	3.8 (1)
C5	6.1 (3)	4.9 (3)	3.6 (3)	1.4 (3)	2.9 (2)	0.5 (2)	4.2 (1)
C6	6.4 (3)	4.4 (3)	2.5 (2)	0.6 (2)	1.7 (2)	-0.4 (2)	4.1 (1)
C7	4.9 (3)	4.7 (3)	2.5 (2)	1.1 (2)	0.7 (2)	1.1 (2)	3.9 (1)

[a] Number in parentheses is the standard deviation of the last significant figure.   [b] Isotropic B value.

Table III. Interatomic Distances (Å) in $Cp_2Mo_2(CO)_4I_2$

Mo–I	2.853 (1)	Mo–C1	1.954 (5)
Mo–I'	2.852 (1)	Mo–C2	1.946 (5)
Mo···Mo'	4.441 (1)	C1–O1	1.155 (6)
I···I'	3.581 (1)	C2–O2	1.156 (6)
Mo–C3	2.250 (5)	C3–C4	1.419 (9)
Mo–C4	2.297 (5)	C3–C7	1.433 (8)
Mo–C5	2.407 (5)	C4–C5	1.404 (9)
Mo–C6	2.395 (5)	C5–C6	1.408 (10)
Mo–C7	2.286 (5)	C6–C7	1.428 (9)

Table IV. Interatomic Angles (deg) in $Cp_2Mo_2(CO)_4I_2$

I–Mo–I'	77.76 (2)	C3–Mo–C4	36.4 (2)
Mo–I–Mo'	102.24 (2)	C3–Mo–C5	58.6 (2)
C1–Mo–C2	75.8 (2)	C3–Mo–C6	59.3 (2)
C1–Mo–C3	92.1 (2)	C3–Mo–C7	36.8 (2)
C1–Mo–C4	85.3 (2)	C4–Mo–C5	34.6 (2)
C1–Mo–C5	113.4 (2)	C4–Mo–C6	58.4 (2)
C1–Mo–C6	143.7 (2)	C4–Mo–C7	60.4 (2)
C1–Mo–C7	127.6 (2)	C5–Mo–C6	34.1 (2)
C2–Mo–C3	91.8 (2)	C5–Mo–C7	58.4 (2)
C2–Mo–C4	124.2 (2)	C6–Mo–C7	35.4 (2)
C2–Mo–C5	148.3 (2)	C4–C3–C7	107.8 (6)
C2–Mo–C6	122.9 (2)	C3–C4–C5	108.0 (5)
C2–Mo–C7	91.36 (2)	C4–C5–C6	109.0 (6)
		C5–C6–C7	107.9 (6)
		C3–C7–C6	107.2 (6)

passing through the iodine and the midpoint of the Mo–Mo bond. The bridging hydride could not be located in the latter structure, but the location of the hydrogen is presumably on the pseudo-C_2 axis opposite the iodine (note the open coordination site at that position in Figures 4 and 5).

One of the most striking differences between the structures of **2** and **8** is found in the Mo–Mo separations. In **2**, this separation is 4.441 Å, consistent with the expectation of no Mo–Mo bond based on the 18-electron rule. The bridging hydride in **8** donates two less electrons than the bridging I⁻ in **2**, and a direct Mo–Mo bond is then expected on the basis of the 18-electron rule. The Mo–Mo distance (3.310 Å) and the acute Mo–I–Mo angle (73.70° in **8** vs. 102.24° in **2**) support the presence of a direct Mo–Mo interaction in **8**.

However, the "normal" Mo–Mo single bond distance in bridged $Mo_2(\mu\text{-}X)$ structures seems to be ca. 3.00 ± 0.05 Å.[23] It has been recognized for some time that hydrogen-bridged metal–metal bonds may be viewed as three-center, 2-electron bonds.[24] Con-

(23) (a) Curtis, M. D.; Han, K. R.; Butler, W. M. *Inorg. Chem.* **1980**, *19*, 2096. (b) Curtis, M. D.; Butler, W. M. *J. Chem. Soc., Chem. Commun.* **1980**, 998. (c) Messerle, L.; Curtis, M. D. *J. Am. Chem. Soc.* **1982**, *104*, 889. (d) Schmid, G.; Boese, R.; Welz, E. *Chem. Ber.* **1975**, *108*, 260.

Table V. Crystal and Data Collection Summary for $Cp_2Mo_2(CO)_4(\mu\text{-}H)(\mu\text{-}I)$ (8)

space group	$P2_1/n$
a, b, c, Å	9.321 (3), 15.131 (6), 11.394 (4)
β, deg	97.94 (3)
V, Å³	1591.6 (10)
Z	4
ρ_{obsd}, g/cm³	2.34
ρ_{calcd}, g/cm³	2.25
crystal dimensions, mm	0.20 × 0.15 × 0.13
radiation	Mo $K\alpha_1$ monochromatized from a graphite crystal
μ, cm⁻¹	34.70
scan speed, deg/min	2.5–12 (variable)
standard reflections	-122, -211, -302
2θ limit, deg	55
total reflections	4308
reflections with $I > 3\sigma$ (I)	2647
R_1	0.063
R_2	0.073
NV	190
NO/NV	13.9
$[\Sigma w(|F_o| - |F_c|)^2/(NO - NV)]^{1/2}$	2.33

Table VI. Fractional Atomic Coordinates for $Cp_2Mo_2(CO)_4(\mu\text{-}H)(\mu\text{-}I)$ (8)

atom	x	y	z
Mo1	-0.0879 (1)	0.1260 (1)	0.3025 (1)
Mo2	0.2413 (1)	0.0815 (1)	0.2411 (1)
I	0.0518 (1)	0.2065 (1)	0.1329 (1)
C1	-0.1431 (12)	0.0016 (8)	0.2745 (10)
O1	-0.1787 (11)	-0.0686 (6)	0.2601 (9)
C2	-0.2498 (12)	0.1304 (8)	0.1732 (11)
O2	-0.3463 (10)	0.1323 (7)	0.0982 (8)
C3	0.3117 (15)	0.0804 (10)	0.4102 (13)
O3	0.3610 (13)	0.0797 (9)	0.5094 (9)
C4	0.3697 (14)	0.1829 (8)	0.2643 (12)
O4	0.4492 (11)	0.2428 (7)	0.2773 (11)
C5	-0.2357 (15)	0.1533 (9)	0.4405 (11)
C6	-0.2027 (15)	0.2366 (9)	0.3934 (11)
C7	-0.0547 (17)	0.2527 (9)	0.4245 (13)
C8	0.0094 (16)	0.1813 (9)	0.4929 (11)
C9	-0.1035 (16)	0.1195 (10)	0.5027 (10)
C10	0.3544 (16)	0.0302 (10)	0.0883 (14)
C11	0.4149 (15)	-0.0130 (10)	0.1943 (15)
C12	0.3023 (20)	-0.0646 (9)	0.2321 (15)
C13	0.1735 (18)	-0.0568 (9)	0.1486 (16)
C14	0.2040 (17)	0.0017 (10)	0.0573 (15)

sistent with this view, the computed Mo–Mo overlap population in **8** is only 0.06.[25] For comparison, overlap populations of around

Table VII. Anisotropic Thermal Parameters for $Cp_2Mo_2(CO)_4(\mu\text{-H})(\mu\text{-I})$ (8)

atom	β_{11}	β_{22}	β_{33}	β_{12}	β_{13}	β_{23}
Mo1	0.0081 (1)	0.0020 (0)	0.0041 (1)	0.0002 (1)	−0.0001 (1)	−0.0001 (0)
Mo2	0.0083 (1)	0.0023 (0)	0.0057 (1)	−0.0000 (1)	0.0011 (1)	−0.0001 (0)
I	0.0116 (1)	0.0028 (0)	0.0066 (1)	−0.0001 (0)	0.0008 (1)	0.0015 (0)
C1	0.0096 (14)	0.0034 (6)	0.0051 (9)	0.0006 (8)	−0.0006 (9)	−0.0001 (6)
O1	0.0178 (16)	0.0022 (4)	0.0125 (11)	−0.0020 (7)	−0.0007 (10)	−0.0005 (5)
C2	0.0086 (14)	0.0036 (6)	0.0066 (10)	0.0004 (8)	0.0010 (10)	−0.0005 (6)
O2	0.0113 (12)	0.0071 (7)	0.0076 (9)	0.0023 (7)	−0.0030 (9)	−0.0008 (6)
C3	0.0115 (17)	0.0048 (7)	0.0086 (13)	0.0010 (9)	0.0012 (12)	−0.0008 (8)
O3	0.0183 (17)	0.0092 (9)	0.0074 (10)	0.0020 (10)	−0.0025 (10)	0.0006 (7)
C4	0.0113 (17)	0.0031 (6)	0.0084 (12)	0.0008 (8)	0.0007 (11)	−0.0003 (7)
O4	0.0136 (14)	0.0046 (6)	0.0159 (14)	−0.0018 (8)	0.0010 (11)	−0.0012 (7)
C5	0.0134 (18)	0.0036 (6)	0.0064 (11)	−0.0003 (9)	0.0012 (11)	−0.0011 (7)
C6	0.0140 (19)	0.0040 (6)	0.0064 (11)	0.0025 (9)	0.0003 (11)	−0.0017 (7)
C7	0.0193 (23)	0.0028 (6)	0.0078 (12)	0.0008 (10)	0.0010 (13)	−0.0012 (7)
C8	0.0164 (20)	0.0036 (6)	0.0048 (9)	0.0007 (10)	−0.0005 (11)	−0.0011 (6)
C9	0.0176 (22)	0.0052 (8)	0.0038 (9)	0.0016 (11)	0.0013 (11)	−0.0005 (7)
C10	0.0125 (19)	0.0047 (7)	0.0113 (15)	0.0003 (10)	0.0051 (14)	−0.0021 (9)
C11	0.0123 (18)	0.0043 (7)	0.0127 (17)	0.0027 (10)	0.0051 (14)	0.0003 (9)
C12	0.0221 (28)	0.0023 (6)	0.0118 (16)	0.0031 (11)	0.0030 (18)	−0.0006 (8)
C13	0.0176 (24)	0.0024 (6)	0.0143 (18)	−0.0008 (10)	0.0058 (17)	−0.0027 (8)
C14	0.0189 (23)	0.0043 (7)	0.0087 (13)	−0.0008 (11)	0.0050 (14)	−0.0027 (8)

Table VIII. Selected Bond Distances (Å) for $Cp_2Mo_2(CO)_4(\mu\text{-H})(\mu\text{-I})$ (8)

Mo1–Mo2	3.310 (2)	C5–C6	1.42 (2)	Mo2–C12	2.29 (1)
Mo1–I	2.759 (1)	C5–C9	1.43 (2)	Mo2–C13	2.39 (1)
Mo1–C1	1.97 (1)	C6–C7	1.40 (2)	Mo2–C14	2.40 (1)
Mo1–C2	1.96 (1)	C7–C8	1.41 (2)	C3–O3	1.16 (2)
Mo1–C5	2.27 (1)	C8–C9	1.42 (2)	C4–O4	1.17 (2)
Mo–C6	2.31 (1)	Mo2–I	2.760 (1)	C10–C11	1.42 (2)
Mo–C7	2.36 (1)	Mo2–C3	1.95 (1)	C10–C14	1.46 (2)
Mo–C8	2.38 (1)	Mo2–C4	1.94 (1)	C11–C12	1.42 (2)
Mo–C9	2.31 (1)	Mo2–C10	2.29 (1)	C12–C13	1.43 (2)
C1–O1	1.12 (1)	Mo2–C11	2.28 (1)	C13–C14	1.42 (2)
C2–O2	1.15 (1)				

Table IX. Selected Bond Angles (deg) for $Cp_2Mo_2(CO)_4(\mu\text{-H})(\mu\text{-I})$ (8)

Mo1–I–Mo2	73.70 (4)	I–Mo2–C3	123.7 (4)
I–Mo1–Mo2	53.17 (4)	I–Mo2–C4	82.1 (4)
I–Mo2–Mo1	53.13 (3)	C3–Mo2–C4	75.8 (6)
I–Mo1–C1	116.6 (3)	C3–Mo2–Mo1	89.3 (4)
I–Mo1–C2	81.2 (4)	C4–Mo2–Mo1	112.5 (4)
C1–Mo1–C2	75.7 (5)	Mo2–C3–O3	176 (1)
C1–Mo1–Mo2	90.0 (3)	Mo2–C4–O4	179 (1)
C2–Mo1–Mo2	119.2 (3)	C10–Mo2–C11	36.2 (5)
Mo1–C1–O1	177 (1)	C11–Mo2–C12	36.3 (6)
Mo1–C2–O2	179 (2)	C12–Mo2–C13	35.5 (6)
C5–Mo1–C6	36.2 (5)	C13–Mo2–C14	34.6 (5)
C6–Mo1–C7	34.8 (5)	C14–Mo2–C10	36.2 (5)
C7–Mo1–C8	34.7 (5)	C14–C10–C11	109 (1)
C8–Mo1–C9	35.3 (5)	C10–C11–C12	107 (1)
C9–Mo1–C5	36.4 (5)	C11–C12–C13	110 (1)
C9–C5–C6	107 (1)	C12–C13–C14	108 (1)
C5–C6–C7	108 (1)	C13–C14–C10	107 (1)
C6–C7–C8	109 (1)		
C7–C8–C9	106 (1)		
C8–C9–C5	109 (1)		

0.3 are found for direct Mo–Mo single bonds, and the computed Mo–H and Mo–I overlap populations in **8** are 0.32 and 0.34, respectively.

(24) For a review, see: (a) Bau, R.; Teller, R. G.; Kirtley, S. W.; Koetyle, T. F. *Acc. Chem. Res.* **1979**, *12*, 176. (b) Doedens, R. J.; Robinson, W. T.; Ibers, J. A. *J. Am. Chem. Soc.*. **1967**, *89*, 4323. (c) Churchill, M. R.; Julis, S. A. *Inorg. Chem.* **1977**, *16*, 1488. (d) Petersen, J. L.; Dahl, L. F.; Williams, J. M. *J. Am. Chem. Soc.* **1974**, *96*, 6610. (e) Wong, K. S.; Scheidt, W. R.; Labinger, J. A. *Inorg. Chem.* **1979**, *18*, 136. Similar conclusions concerning the nature of M–H–M bonds (open 3c–2e) have been drawn recently by: DeKock, R. L.; Wong, K. S.; Fehlner, T. P. *Inorg. Chem.*, **1982**, *21*, 3203.

(25) The calculations were performed with R. Hoffmann's EHMO program, ICON8, using the weighted H_{ij} formalism described in: (a) Ammeter, J. H.; Burgi, H. B.; Thibeault, J. C.; Hoffmann, R. *J. Am. Chem. Soc.* **1978**, *100*, 3686. The parameters used are listed in ref 31. The details of these and related computations will be published elsewhere.
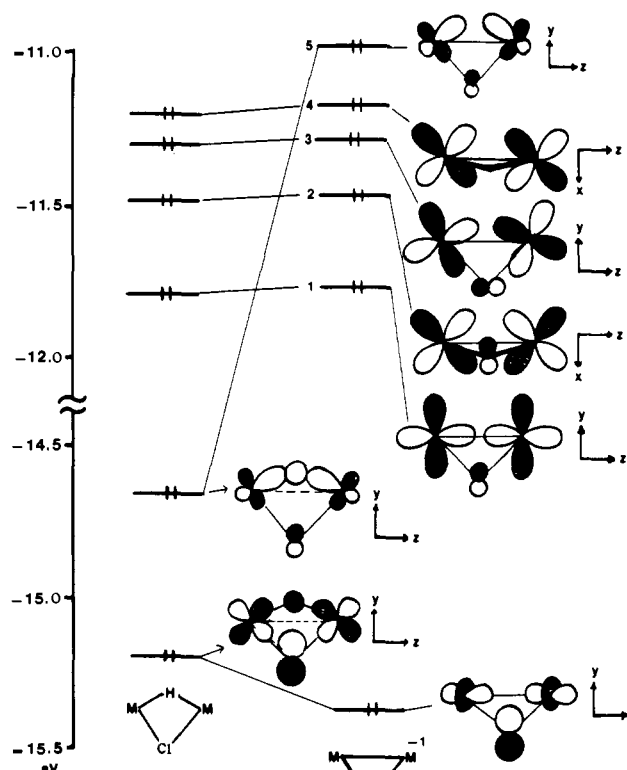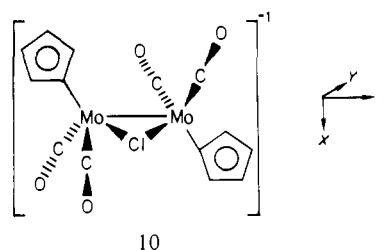
Figure 6. Corresponding molecular orbitals of $Cp_2Mo_2(CO)_4(\mu\text{-Cl})^-$ and $Cp_2Mo_2(CO)_4(\mu\text{-H})(\mu\text{-Cl})$ as computed by the EHMO method. The tie lines connect orbitals of corresponding bonding properties and are not meant to indicate a strict symmetry correlation.

The effect of protonating the Mo–Mo single bond of the Cl⁻-bridged complex **10** is dramatically shown in Figure 6.

10

Orbitals lower in energy than −14 eV are primarily ligand-centered, metal–ligand bonding MO's. Those between 11 and

2692 *J. Am. Chem. Soc., Vol. 105, No. 9, 1983*

Curtis et al.

12 eV are primarily metal centered, with small admixtures of metal–ligand antibonding character. With respect to M–M bonding, the orbitals labeled 1–4 in Figure 6 can be classified as σ, π, σ^*, and π^*, respectively. In addition, the HOMO (orbital 5) is a σ bond, bent out in the direction of the "vacant" coordination site opposite the bridging chloride. The net M–M bond order in **10** is thus assigned a value of 1.0, in accord with the 18-electron rule, which demands a Mo–Mo single bond.

It is this HOMO that is protonated to give the $(\mu\text{-H})(\mu\text{-Cl})$ adduct, **3**. The energy of this orbital drops to about −14.6 eV and is properly classified as a three-center, 2-electron MO which is mainly Mo–H bonding. This leaves orbitals 1–4 for direct metal–metal bonding, but these orbitals give a net bond order of 0. The computed Mo–Mo overlap populations for **3** and **10** (0.09 and 0.29, respectively) are in accord with this analysis. The population analysis would suggest an "open" three-center bond description is more appropriate than a "closed" three-center bond, which entails direct M–M bonding.[24e]

The Mo–I bond distances in the two compounds, **2** and **8**, are also significantly different, having the values 2.853 (1) and 2.760 (1) Å, respectively. Reported Mo–I distances range from 2.76 Å in $CpMo(CO)_2(PBu_3)I^{26}$ to 2.86 Å in $[(t\text{-BuNC})_3MoI]I,^{27}$ but are clustered around 2.85 Å.[28–30]

EHMO analysis of the bonding in **2** and **8** gave no clear indications of a dominant interaction that would explain the differences in the Mo–I bond lengths in the two compounds. For a constant Mo–I distance, the bridging iodine moves out from the Mo–Mo bond axis as the Mo–Mo bond distance decreases. At short Mo–Mo separations, metal–metal repulsion sets in, while at large M–M separations, I–I repulsions become important in destabilizing the structure. At intermediate distances, the iodine atoms may traverse the nodal surfaces of the metal d orbitals and enter regions that give rise to poor Mo–I bonding. Adjustments in the Mo–I bond lengths may then occur in order to move the iodines off these nodal surfaces. The complex interplay of all three of these interactions determines the best (i.e., lowest energy) structure.

One possible explanation of the shorter Mo–I bonds in the H–I adduct involves the "cross-ring" interactions. At a Mo–Mo separation of 4.44 Å and a Mo–I bond distance of 2.80 Å, the overlap of the iodine p_y orbitals in **2** is 0.111 as compared to an I–H overlap of only 0.05 in **8** (Mo–Mo distance = 3.310). The I–I overlap population in **2** is −0.03 vs. only −0.002 for the H–I overlap population in **8**. Thus, in **2**, the iodines back off to relieve I–I repulsions, but the iodine in **8** moves in to increase Mo–I bonding.

The local environments of the Mo atoms in **2** and **8** are of the four-legged piano stool type, $CpM(CO)_2LL'$. This class of complex was recently analyzed by Hoffmann and co-workers[31] using the EHMO method. These workers observed that the best π acceptors in $CpMoL_4$ complexes tend to be under the middle of a C–C bond of the Cp ligand. In **2** and **8**, the carbonyls are the best π acceptors and they do, in fact, lie under the C–C bonds. Figure 7 indicates the Mo–C(Cp) distances in **2** and **8** in relation to the positions of the CO and I or H ligands. As can be seen, the two Mo–C distances opposite the carbonyls are significantly longer than the other three Mo–C distances, the respective averages being 2.39 and 2.28 Å.

The division of the Mo–C(Cp) distances into sets of short and long is a manifestation of the trans influence commonly found in square-planar complexes. This trans influence repels the Cp carbon atoms in the trans positions, giving the Cp ring a significant tilt as shown in Figure 7c. In $CpML_4$, only weak δ interactions between the Cp-ligand e_2 orbitals and the metal orbitals can give rise to tilting of the Cp ring, and these distortions are calculated to be quite small.[31]
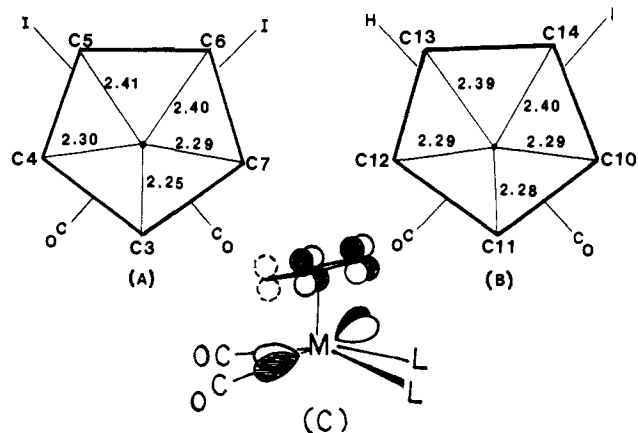

Figure 7. (a) Mo–C(Cp) distances of **2** in relation to their spatial orientation relative to the carbonyl and iodine ligands. (b) As in (a) for complex **8**. The averages of the two equivalent Mo–Cp distances are displayed. (c) Side view of the Cp tilt and the metal hybrid MO used in Mo–CO σ bonding and Mo–Cp π bonding.

In the present instance of $cis\text{-}CpMo(CO)_2L_2$ complexes, the basis for the tilt seems to lie with the π interactions. The same d_π orbital used in σ bonding to the CO ligands is also used in a π interaction with the p_π orbitals of the two distal Cp carbons (see Figure 7c). Because of the stronger M–CO bonding, this d_π orbital is polarized by admixture of metal p orbitals toward the CO and away from the Cp. The bonding to these two ring carbons is then weakened, giving rise to the observed tilt. Even when all the M–C(Cp) distances are equal, the calculated overlap populations of the M–C(Cp) bonds are typically 0.13 for the three bonds that become shorter vs. 0.12 for the two bonds that become longer.

Conclusions

Electrophilic addition of HX or X_2 (X = Cl, I) to the Mo≡Mo triple bond in $Cp_2Mo_2(CO)_4$ gives the complexes $M_2(\mu\text{-H})(\mu\text{-X})$ and M_2X_2, respectively. There are several structural alternatives open to these dihalides. Both the diiodide and dichloride exhibit at least two structures, one of which was shown by X-ray diffraction to have the $M_2(\mu\text{-I})_2$ structure. Work is continuing on synthesizing the complete series of the halides of $Cp_2M_2(CO)_4$ (M = Mo, W) and establishing their structures. In addition to their theoretical interest, these complexes serve as convenient starting materials for a variety of organometallic products.

Experimental Section

Manipulation of air-sensitive materials was achieved with standard Schlenk techniques or in a Vacuum Atmospheres glovebox filled with helium and equipped with a freezer maintained at −40 °C. Toluene, ether, and THF were dried over sodium benzophenone, methylene chloride over P_4O_{10}, and aliphatic hydrocarbons over 4-Å molecular sieves. The ethers, toluene, and CH_2Cl_2 were distilled immediately prior to use and the hydrocarbon solvents were deaerated by bubbling N_2 through them.

IR spectra were recorded on Perkin-Elmer 457 or Beckman IR 4240 spectrometers. Routine NMR spectra were recorded on Varian T-60 instruments. Higher field spectra were recorded on a Bruker 360 MHz, a JEOL JNM FS-100, or a JEOL FX-90Q spectrometer. Mass spectra were obtained on an AEI MS902 or a Finnigan 4023 GC/MS system. Elemental analyses were performed by Galbraith Laboratories, Knoxville, TN.

The compounds $Cp_2Mo_2(CO)_4,^7$ $Cp_2Mo_2(CO)_4(\mu\text{-I})_2,^7$ and $PhICl_2^{32}$ were obtained by published procedures. Crystallographic quality crystals of the diiodide **2** were obtained by saturating a toluene solution at −10 °C with the red-brown solid obtained as in ref 7 and then allowing this solution to stand in contact with excess solid **2** for 10 days and then filtering the cold suspension under N_2.

(μ-Hydrido)(μ-Iodo)bis(cyclopentadienyldicarbonylmolybdenum) (8). One millimole (0.43 g) of $Cp_2Mo_2(CO)_4$ (**1**) was placed in a 100-mL side-arm flask and dissolved in 20 mL of toluene under N_2. A septum was placed over the flask and the contents were then cooled to −78 °C

(26) Fenn, R. H.; Cross, J. H. *J. Chem. Soc. A* **1971**, 3312.
(27) Lewis, P. F.; Lippard, S. J. *Inorg. Chem.* **1972**, *11*, 621.
(28) Mauby, A.; Pringle, G. E. *J. Inorg. Nucl. Chem.* **1972**, *34*, 525.
(29) Adams, R. D.; Chodosh, D. F. *J. Am. Chem. Soc.* **1977**, *99*, 6544.
(30) Hardy, A. D. U.; Sim, G. A. *J. Chem. Soc., Dalton Trans.* **1972**, 1900.

(31) Kubacek, P.; Hoffmann, R.; Halvas, Z. *Organometallics* **1982**, *1*, 180.
(32) Lucas, H. J.; Kennedy, E. R. "Organic Syntheses"; Wiley: New York, 1955; Collect. Vol. III, p 482.

with the side arm closed. The HI(g) (39 mL, 1.5 mmol) was then injected into the solution with a plastic, disposable syringe. The solution was then allowed to warm to 0 °C and stirred for 2 h. The mixture was then filtered cold and the filtrate concentrated to a volume of ca. 10 mL under vacuum. To the concentrated filtrate was added 10 mL of heptane and this mixture was then cooled to −20 °C overnight. The resulting mixture was filtered cold to give a black crystalline solid, which was washed with cold pentane and dried under vacuum; yield 54%. In solution, the compound is reddish in color and is stable under N_2 for several days. In the solid state, the compound is stable indefinitely under N_2 and can be weighed in air with no apparent decomposition; ν_{CO} 1940, 1855 (KBr); NMR (C_6D_6) δ 4.72 (Cp), −11.45 (hydride). Anal. Calcd for $C_{14}H_{11}IMo_2O_4$: C, 29.90; H, 1.96; I, 22.59. Found: C, 30.05; H, 1.78; I, 22.98.

Bis(μ-iodo)bis(cyclopentadienyldicarbonylmolybdenum) (2) from 1 and HI. The procedure was the same as described above except that 90 mL (3.8 mmol) of gaseous HI was added to the solution of $Cp_2Mo_2(CO)_4$. After warming to 0 °C from −78 °C the reaction mixture was filtered while cold to yield some brown solid, later shown to be $Cp_2Mo_2(CO)_4$-$(\mu\text{-I})_2$ (2). The filtrate was treated as in the previous preparation to give further brown solid, identical with $Cp_2Mo_2(CO)_4(\mu\text{-I})_2$ prepared from 1 and I_2.[7]

(μ-Chloro)(chlorocyclopentadienyldicarbonylmolybdenum)(cyclopentadienyldicarbonylmolybdenum)(*Mo–Mo*) (6) from 1 and HCl. Hydrogen chloride gas was bubbled through a solution of 0.43 g (1.0 mmol) of 1 in 20 mL of toluene for 2–3 min (a protective blanket of N_2 was maintained). During this time, the color of the solution changed from red brown to a muddy brown. The mixture was then immediately cooled to −78 °C and subjected to vacuum in order to remove excess HCl. The solution was then warmed to room temperature under vacuum until approximately half the toluene had distilled out. Heptane (8 mL) was then added and the mixture placed in a −20 °C freezer overnight. Filtration yielded a black, crystalline solid, which is stable for days under N_2. In solution at room temperature, decomposition is evident after 5 min, but decomposition occurs more slowly as the temperature is lowered; ν_{CO} 1995, 1940, 1900, 1855 (sh) cm^{-1}; NMR (C_6D_6) δ 4.95, 4.92 (Cp, 1:1). Anal. Calcd for $C_{14}H_{10}Cl_2Mo_2O_4$: C, 33.30; H, 1.98; Cl, 14.00; Mo, 38.10. Found: C, 33.34; H, 2.03; Cl, 14.69; Mo, 39.21.

Synthesis of 6 from 1 and PhICl$_2$. One millimole (0.43 g) of $Cp_2Mo_2(CO)_4$ (1) was dissolved in 20 mL of toluene in a 100-mL Schlenk flask. The solution was cooled to −50 °C and 1 mmol (0.28 g) of $PhICl_2$ was then added. After 5 min, the color of the reaction mixture had changed from red brown to dark brown. After stirring at −50 °C for 1.5 h, the mixture was filtered, giving a brown solid and a dark filtrate. The volume of the filtrate was approximately halved by pumping off the solvent in vacuo, and 10 mL of heptane was then added. Allowing this mixture to stand at −20 °C overnight gave black crystals, the NMR spectrum of which indicated the presence of 6 and unreacted 1. One recrystallization from PhMe/heptane at −20 °C gave pure 6, identical with that described in the previous preparation.

Reaction of 1 with Cl$_2$. One millimole of $Cp_2Mo_2(CO)_4$ (1) in toluene (20 mL) at −78 °C was allowed to react with 40 mL (1.6 mmol) of Cl_2. An immediate reaction ensued with the formation of a brown precipitate. The mixture was allowed to warm to 0 °C and filtered to give a brown solid, and the solvent was removed from the filtrate in vacuo (no crystalline solid was obtained with the usual workup described above). The IR spectrum of the initial brown solid has ν_{CO} peaks at 2100, 2070, 2030, 1950, 1925, 1900, and 1890 cm^{-1}, suggesting the presence of $CpMo(CO)_2Cl_3$ (2104, 2065 cm^{-1}),[33] possibly some $Cp_2Mo_2(CO)_6$, and other unidentified substances. NMR and IR spectra of the residue from the filtrate indicated the presence of $CpMo(CO)_2Cl_3$ (δ 5.7),[33] 6 (ca. 10%), and $CpMo(CO)_3Cl$.

Reaction of 2 and 8 with Aluminum Hydrides. A toluene solution of Vitride ($Na[H_2Al(OCH_2CH_2OCH_3)_2]$) containing 1 mmol of the aluminum hydride was added to a solution of 0.69 g (1 mmol) of 2 in THF at −40 °C. As the solution warmed to room temperature, the color changed from red-violet to cherry red. This solution was stirred for 1 h and then filtered, yielding a pink solid, which was discarded. The solvent was stripped from the filtrate and the resultant solid was extracted with 15–20 mL of toluene, leaving a purple solid on the filter and giving a red-brown filtrate. The purple solid contained 48% I but only 7% Mo and was not identified. The toluene was pumped off the filtrate and the residue was identified by NMR as a mixture of 1 and 8.

With $LiAlH(O\text{-}t\text{-Bu})_3$ as the hydride source, the reaction was cleaner. Thus, 1.03 g (1.5 mmol) of 2 in 30 mL of THF at −40 °C was allowed to react with added, solid $LiAlH(O\text{-}t\text{-Bu})_3$ (0.39 g, 1.5 mmol). The mixture was allowed to warm to room temperature and the THF stripped under vacuum. The resulting residue was extracted with toluene and this

mixture was filtered through a *fine*-porosity frit to give a purple solid (found: C, 31.17%; H, 5.36%; Mo, 10.66%; Al, 3.45%; I, 32.74%) and a reddish filtrate. The volume of the filtrate was reduced to ca. 10 mL by removal of toluene under vacuum, 10 mL of heptane was added, and the mixture was held at −20 °C overnight. A black solid crystallized and was shown by IR, NMR, and elemental analysis to be $Cp_2Mo_2(CO)_4$-$(\mu\text{-H})(\mu\text{-I})$ (42%). Anal. Calcd for $C_{14}H_{11}IMo_2O_4$: C, 29.90; H, 1.96. Found: C, 29.66; H, 2.13.

In a similar fashion, 0.23 g (0.41 mmol) of $Cp_2Mo_2(CO)_4(H)(I)$ (8) was allowed to react with 0.41 mmol of $LiAlH(O\text{-}t\text{-Bu})_3$ in THF at −40 °C. After warming to room temperature, the mixture was stirred for 1 h, the THF was then stripped off under vacuum, the residue taken up in toluene, and this solution filtered through a fine-porosity frit. Removal of the toluene under vacuum gave a red-brown solid, which was shown by NMR to be $Cp_2Mo_2(CO)_4$ (75%) and unreacted 8 (25%).

Reaction of 8 and Ethylene. Into a thick-walled, glass reaction vessel (20-mL capacity) equipped with a magnetic stir bar, pressure gauge, and inlet septum was placed 0.181 g (0.32 mmol) of 8. The flask was evacuated and back-filled three times with ethylene. The solvent, 4 mL of chlorobenzene, was then syringed into the vessel through the septum and the ethylene pressure was then increased to 45 psig (ca. 4 atm). The solution was then stirred at 70 °C for 13 h. The pressure was then released and the solution transferred by syringe to a Schlenk flask. The volatiles were removed by a trap-to-trap distillation. A GC/MS showed only one peak (other than solvent) and the mass spectrum matched the library spectrum of 3-pentanone. This material was isolated by preparative GC and its NMR spectrum (δ 2.27 (q), 1.19 (t), $J = 7.2$ Hz, 2:3 ratio) matched that of authentic 3-pentanone. Using a known amount of *n*-octane internal standard, the GC-determined yield of 3-pentanone was 0.061 mmol (38% based on available metal hydride). The largest component of the soluble metal species was $CpMo(CO)_3I$, identified by comparison of its IR and NMR spectra with authentic material.[34] The use of C_6D_6 or C_7D_8 as solvent did not affect the results. Under identical conditions except that the ethylene was replaced with nitrogen, 95% of the original 8 was still present. With CO or CO/H_2 atmospheres, no decomposition was noted under these conditions.

With 1-hexene, only isomerization to 2- and 3-hexenes was observed (the olefins were identified by NMR and GC/MS). Decomposition of 8 to $CpMo(CO)_3H$,[35] $CpMo(CO)_3I$, and dark, insoluble material was also noted.

Synthesis of Bis(μ-iodo)bis[(methylcyclopentadienyl)dicarbonylmolybdenum] (5). A solution of 0.81 g (3.2 mmol) of I_2 in 100 mL of toluene was added dropwise over the course of 1 h to a stirred solution of 1.5 g (3.2 mmol) of $Cp'_2Mo_2(CO)_4$ in 20 mL of toluene in a 250-mL Schlenk flask. An acetone bath was maintained at ca. −20 °C by periodic addition of dry ice. After the addition was complete, the mixture was stirred at −20 °C for 45 min and then filtered while still cold. The filtrate was concentrated in vacuo and placed in a −20 °C freezer overnight. The cold mixture was then filtered to give purple, crystalline Cp'_2Mo_2-$(CO)_4(\mu\text{-I})_2$: ca. 60% yield; mp 105–110 °C dec; ν_{CO} (KBr) 1945, 1860, 1850, 1830 cm^{-1}; NMR (C_7D_8) A_2B_2 pattern centered at δ 4.61, $\Delta\delta =$ 30.5 Hz, $J = 2.1$ Hz. Anal. Calcd for $C_{16}H_{14}I_2Mo_2O_4$: C, 26.83; H, 1.96; Mo, 26.89; I, 35.47. Found: C, 26.27; H, 1.88; Mo, 26.99; I, 36.29. The $(\mu\text{-I})_2$ structure assigned to this complex has been confirmed by an X-ray structure determination.[36]

Reaction of $Cp_2Mo_2(CO)_4$ and HCl. In a 100-mL Schlenk flask was placed 0.9 g (2.1 mmol) of $Cp_2Mo_2(CO)_4$ (1) and 20 mL of dry CH_2Cl_2. A 133-mL flask filled to 285 torr with HCl (2.16 mmol) was then attached to the Schlenk flask. The CH_2Cl_2 solution was then frozen in liquid N_2 and the Schlenk flask evacuated, sealed, and then allowed to warm to −20 °C. The stopcock to the HCl flask was then opened, allowing the HCl to enter the reaction flask. After stirring for 2 h at −15 to −11 °C, 15 mL of heptane was added and some of the CH_2Cl_2 pumped off at room temperature under vacuum. Filtration gave a red-brown solid (shown to be unreacted 1). The filtrate was cooled to −20 °C for 8 h to give a dark-red, crystalline solid, shown by IR and NMR to be a mixture of $Cp_2Mo_2(CO)_4$ (ν_{CO} 1890, 1850 cm^{-1}; NMR δ 4.63), $CpMo(CO)_3Cl$ (ν_{CO} 2040, 1980, 1960 cm^{-1}; NMR δ 4.55),[35] and smaller amounts of $Cp_2Mo_2(CO)_4(Cl)_2$ (NMR δ 4.95, 4.92) and $Cp_2Mo_2(CO)_4(H)(Cl)$ (NMR δ 4.72).

When excess HCl is bubbled through a solution of 1 in dry CH_2Cl_2, 1 is totally consumed in less than 5 min to give mostly an intractable brown powder and traces of $CpMo(CO)_3Cl$ and $Cp_2Mo_2(CO)_4(Cl)_2$.

---

(33) Green, M. L. H.; Lindsell, W. E. *J. Chem. Soc. A* 1967, 686.

(34) Manning, A. R. *J. Chem. Soc. A* 1967, 1984.
(35) Piper, T. S.; Wilkinson, G. *J. Inorg. Nucl. Chem.* 1956, 3, 104.
(36) Curtis, M. D., Fotinos, N. F., unpublished results.

Further Studies of the Dimeric β-Linked "Face-to-Face Four" Porphyrin: FTF4

James P. Collman,[*1a] **Fred C. Anson,**[*1b] **Craig E. Barnes,**[1a] **C. Susana Bencosme,**[1a] **Thomas Geiger,**[1b] **Eric R. Evitt,**[1a] **Robert P. Kreh,**[1a] **Kurt Meier,**[1a] **and Roger B. Pettman**[1a]

Contribution from the Department of Chemistry, Stanford University, Stanford, California 94305, and the Arthur Amos Noyes Laboratories, Division of Chemistry and Chemical Engineering, California Institute of Technology, Pasadena, California 91125. Received August 9, 1982

Abstract: High-pressure liquid chromatographic analysis of the previously reported cofacial porphyrin dimer (FTF4), which is linked by two four-atom amide bridges in transverse β-pyrrolic positions, revealed that it contained two minor impurities. ^{1}H NMR, UV–visible, and mass spectroscopic analyses showed these to be two related meso monochlorinated face-to-face porphyrin dimers. Rotating ring–disk voltammetric measurements of the dicobalt derivatives revealed that the chlorinated dimers were better catalysts for the four-electron reduction of O_2 to H_2O than the corresponding nonfunctionalized parent molecule. Reinvestigation of the origin of the contaminants led to a new synthetic route to pure FTF4.

When adsorbed on edge-plane pyrolytic graphite, the dicobalt derivative of the β-linked porphyrin dimer with two four-atom amide bridges $(Co_2(FTF4))$[2,3] (Figure 1) catalyzes the four-electron reduction of oxygen to water at ca. 0.68 V vs. NHE at pH less than 3.5,[5] with a turnover rate of ca. 400 dioxygen molecules per second per catalyst site.[6] At present, $Co_2(FTF4)$ is the only synthetic compound that displays such remarkable activity. Platinum, the most effective metal catalyst, operates at 0.63 V vs. NHE in acid, with a turnover rate of 0.3–5 dioxygen molecules per second per platinum site.[7]

As shown in Figure 1, the β-linked dimer can exist in two possible isomeric forms, syn and anti, depending on the relative orientation of the two rings. In turn, each of these two diastereomers can exist as an enantiomorphic pair. Attempts to resolve these two possible diastereomers using high-pressure liquid chromatography (HPLC) led to the surprising result that the

original FTF4 dimer[6] (prepared as shown in Figure 2) was actually contaminated with two minor impurities. These experiments (vide infra) showed that only one of the two possible diastereomers was present. Apparently, the kinetically controlled binary cyclophane formation affords only the less hindered anti isomer. In dealing with a multicomponent mixture, it is always possible that the observed catalysis is derived from the activity of a minor component while the major component—the assumed catalyst— is inactive. It was, therefore, essential for each of the components of the mixture to be isolated, characterized, and studied for catalytic activity in the reduction of O_2. This work presents the results of such a study and also describes two independent synthetic pathways to pure FTF4.

Results and Discussion

High-Pressure Liquid Chromatography. The HPLC analysis of the original FTF4,[4] prepared as shown in Figure 2, revealed that it had two minor impurities (ca. 8%) which exhibited optical spectra characteristic of these cofacial porphyrin dimers. The pure FTF4 and the two minor contaminants were separated on an analytical Whatman partisil 10 column with 85:10:5 CH_2Cl_2–CH_3CN–CH_3OH as eluent. The resulting chromatogram is shown in Figure 3. Through repeated injections, a few hundred micrograms of fractions a, b, and c were isolated and characterized by mass spectrometry and ^{1}H NMR and UV–visible spectroscopy.

In order to determine the source of these impurities, we analyzed the two starting reagents for the FTF4 coupling (Figure 2), the C2 di-*p*-nitrophenyl ester **3** and the C1 diamine **5** by using HPLC. The chromatogram of compound **3** showed a single component. Analysis of the C1 diamine **5** as its ditrityl derivative, however, revealed the presence of two impurities (Figure 4). It therefore seemed likely that these were the origin of the FTF4 impurities.

Mass Spectra. Both field-desorption (FD) and electron-impact (EI) mass spectra of the HPLC fractions a, b, and c were obtained. Perfluorokerosene was used as a mass marker, with an upper limit at m/e 1023. Each fraction was checked from m/e 400 to well beyond m/e 1023.

Fraction c gave a very strong molecular ion at m/e 982, which is consistent with the molecular weight calculated for FTF4 $(C_{62}H_{66}N_{10}O_2)$. Both the FD and EI spectra of fraction c fit the

(1) (a) Stanford University (this paper was abstracted from the Ph.D. Thesis of C.S.B., Stanford University, 1982). (b) California Institute of Technology.

(2) Abbreviations used in this paper: FTF4, free-base face-to-face porphyrin depicted in Figure 1; NHE, normal hydrogen electrode; SCE, standard calomel electrode; HPLC, high-pressure liquid chromatography; C2 diethyl ester, C1 diamine, and C2 di-*p*-nitrophenyl ester are the porphyrin monomers **1**, **5**, and **3** in Figure 2; C2 hydrazide is the porphyrin monomer **4** depicted in Figure 9; FD, field-desorption mass spectrometry; EI, electron-impact mass spectrometry; OEP, octaethylporphyrin; THF, tetrahydrofuran; TLC, thin-layer chromatography.

(3) A series of face-to-face porphyrins has been synthesized by Collman and co-workers as an approach to the design of catalysts for the rapid four-electron reduction of O_2 to H_2O. For an account, see ref 4, 5, and 6, and references cited therein.

(4) Collman, J. P.; Anson, F. C.; Bencosme, S.; Chong, A.; Collins, T.; Denisevich, P.; Evitt, E.; Geiger, T.; Ibers, J. A.; Jameson, G.; Konai, Y.; Koval, C.; Meier, K.; Oakley, R.; Pettman, R.; Schmittou, E.; Sessler, J. In "Organic Synthesis Today and Tomorrow" (IUPAC); Trost, B. M., Hutchinson, C. R., Eds.; Pergamon: Oxford, 1981; pp 29–45.

(5) Collman, J. P.; Marrocco, M.; Denisevich, P.; Koval, C.; Anson, F. C. *J. Electroanal. Chem. Interfacial Electrochem.* **1979**, *101*, 117–122.

(6) (a) Collman, J. P.; Denisevich, P.; Konai, Y.; Marrocco, M.; Koval, C.; Anson, F. C. *J. Am. Chem. Soc.* **1980**, *102*, 6027–6036. (b) Durand, R. R., Jr.; Bencosme, C. S.; Collman, J. P.; Anson, F. C. *J. Am. Chem. Soc.*, fourth paper of four in this issue.

(7) Damjanovic, A.; Genshaw, M. A.; Bockris, S. O'M. *J. Electrochem. Soc.* **1967**, *114*, 1108.